J Appl Electrochem (2014) 44:917–926
DOI 10.1007/s10800-014-0711-1

RESEARCH ARTICLE

Efficiency enhancement of dye-sensitized solar cells with PAN:CsI:LiI quasi-solid state (gel) electrolytes

T. M. W. J. Bandara · W. J. M. J. S. R. Jayasundara · H. D. N. S. Fernado · M. A. K. L. Dissanayake · L. A. A. De Silva · P. S. L. Fernando · M. Furlani · B.-E. Mellander

Received: 8 April 2014 / Accepted: 23 June 2014 / Published online: 16 July 2014

Abstract While many attempts have been made in the recent past to improve the power conversion efficiencies of dye-sensitized solar cells (DSSCs), only a few reports can be found on the study of these cells using binary iodides in the gel polymer electrolyte. This paper reports the effect of using a binary mixture of (large and small cation) alkaline salts, in particular CsI and LiI, on the efficiency enhancement in DSSCs with gel polymer electrolytes. The electrolyte with the binary mixture of CsI:LiI = 1:1 (by weight) shows the highest ionic conductivity 2.9×10^{-3} S cm^{-1} at 25 °C. DC polarization measurements showed predominantly ionic behavior of the electrolyte. The density of charge carriers and mobility of mobile ions were calculated using a newly developed method. The temperature dependent behavior of the conductivity can be understood as due to an increase of both the density and mobility of charge carriers. The solar cell with only CsI as the iodide salt gave an energy conversion efficiency of ~3.9 % while it was ~3.6 % for the cell with only LiI. However, the electrolyte containing LiI:CsI with mass ratio 1:1 showed the highest solar cell performance with an energy conversion efficiency of ~4.8 % under the irradiation of one Sun highlighting the influence of the mixed cation on the performance of the cell. This is an efficiency enhancement of 23 %.

Keywords Quasi-solid electrolyte · Dye-sensitized · Solar cell · Binary iodide mixture · Charge carrier

T. M. W. J. Bandara (✉) · H. D. N. S. Fernado · P. S. L. Fernando
Department of Physical Sciences, University of Rajarata, Mihintale, Sri Lanka
e-mail: awijendr@yahoo.com

T. M. W. J. Bandara · M. Furlani · B.-E. Mellander
Department of Applied Physics, Chalmers University of Technology, Gothenburg, Sweden

W. J. M. J. S. R. Jayasundara · M. A. K. L. Dissanayake
Postgraduate Institute of Science, University of Peradeniya, Peradeniya, Sri Lanka

M. A. K. L. Dissanayake
Institute of Fundamental Studies, Hantana Road, Kandy, Sri Lanka

L. A. A. De Silva
Department of Physics, University of West Georgia, Carrollton, GA 30118, USA

1 Introduction

The solar cell is an extremely important device and a candidate to fulfill the future energy requirement since solar energy is a clean, freely available, and limitless source of energy compared to other traditional energy sources. Consequently, low-cost quasi-solid-state dye-sensitized solar cells (DSSCs) have drawn the attention of the research community recently as a promising contender for energy conversion owing to their stability compared to liquid-based cells, even though efficiencies are lower. In addition, easy fabrication and low production cost are additional advantages of DSSCs [1, 2].

A DSSC typically consists of a dye-adsorbed photoelectrode layer on fluorine doped tin oxide (FTO) glass substrate as a working electrode, a Pt-coated counter electrode, and an electrolyte containing a redox couple such as I^-/I_3^- [3, 4] or Co^{+2}/Co^{+3} [5]. The photo-active part in a DSSC is the photoelectrode, in this case the dye-sensitized porous TiO_2 anode. Under the irradiation of sunlight, dye molecules excite and inject electrons into the conduction band of the semiconductor. For an effective

function of DSSC, these excited electrons should be injected into the conduction band of the semiconductor before recombination takes place. In order to generate electricity from the DSSC, the electrons need to pass through four interfaces: dye/TiO_2, TiO_2/FTO, electrolyte/counter electrode, and dye/electrolyte. Effective charge transport across thesse interfaces is therefore extremely important in order to improve the efficiencies in DSSCs.

The electrolyte, as one of the key components of DSSC, should assist not only the charge transport between the two electrodes through the electrolyte but also should provide an efficient charge transfer at the interfaces. It has been established that the size of the cation would influence the injection rates of the electrons from the excited dye molecules to the conduction band of TiO_2 [6]. In particular, smaller cations provide a higher rate for the electron injection from dye to TiO_2 layer. For instance, Kelly et al. [7] have shown that the magnitude of electron injection yields of the dye varies with the charge-to-radius ratio of the cation in the electrolyte and that quantum yields of charge injection decrease in the sequence $Ca^{2+}>Sr^{2+}\sim Ba^{2+}>Li^{+}>Na^{+}>K^{+}=Rb^{+}\sim Cs^{+}\sim Bu_4N^{+}$ using acetonitrile-based liquid electrolytes. Our group also has studied and reported the cation size effect in DSSCs in several recent publications, in particular the quaternary ammonium cation series [8, 9].

Electrons injected from the dye to TiO_2 diffuse to the conducting glass substrate through TiO_2 in order to reach the counter electrode; thus, an efficient diffusion of electrons through the nano-structured TiO_2 is very important for obtaining a higher efficiency. The adsorption or the intercalation of cations on TiO_2 changes the number of electron trap states or the energy level of the trap states, and thus, the diffusion coefficient of electrons depends on the cation nature. It is evident that the presence of smaller cations assists the internal electron conduction of the mesoporous TiO_2 layer due to trap filling [9–11]. Electron transport in TiO_2 correlates with ionic motion in the electrolyte. The electric field generated due to the charge imbalance created by electron transfer drags the cations in the electrolyte and polarizes the electrolyte [12]. This behavior can be explained by ambipolar diffusion [12]. Higher ambipolar diffusion coefficient (D_{ambi}) is shown by larger cations such as tetrabutylammonium (Bu_4N^{+}) and dimethylhexylimidazolium cation ($DMHI^{+}$) at low concentrations. Smaller Li^{+} ion has shown low D_{ambi} for low concentrations which rapidly increases with increasing Li^{+} concentration [10].

Since the major role of the electrolyte in a DSSC is to provide charge transport between the cathode and the dye-coated TiO_2 photo-anode, a higher conductivity for the redox species is important. Although liquid electrolyte-based dye-sensitized solar cells reach power conversion efficiencies of about 11 % [4, 13] with I^{-}/I_3^{-} redox couple and about 12 % with Co^{+2}/Co^{+3} redox couple, the liquid electrolytes limit the practical applications of DSSCs because the liquid can evaporate and leak when the cell is imperfectly sealed, and more generally, the side reactions may worsen cell performance [3, 4]. To overcome these problems, many efforts have been focussed on developing quasi-solid state (gel) polymer electrolytes because of their easy fabrication, mechanical flexibility, low cost, and reasonably good stability [3, 4, 14]. The conduction of the iodide ions in the electrolyte plays an important role in the performance of the cell, and it is also important to understand the effect of the incorporated cations. Several groups have discussed the role of cations in electrolytes on the light-to-electricity conversion process of DSSCs [15–17]. However, very few researches have focused exclusively on cation effects on DSSC performance [6, 9, 18]. In our previous work on DSSCs, the effect of the cations on the efficiency of quasi-solid state DSSCs was studied by using binary iodide salts having a small size alkaline cation along with a larger quaternary ammonium ion [9, 15]. In these studies, the presence of binary iodide salts in the electrolyte has clearly shown an efficiency enhancement in respective DSSCs. Therefore, in order to fabricate efficient DSSCs, a redox couple electrolyte made of a binary iodide salt mixture consisting of small and large cations appears to be important.

To the best of our knowledge, there are no reports in the literature on dye-sensitized solar cells using quasi-solid state (gel) electrolytes containing a binary alkaline iodide system. It is interesting to study this binary alkaline iodide system since most of the quasi-solid state electrolytes used in DSSCs composed of a single alkaline iodide salt or binary systems containing quaternary ammonium salts or ionic liquids [1, 9]. Therefore, in this work, polyacrylonitrile-based gel electrolytes were made with CsI (iodide salt with a large cation) and LiI (iodide salt with a small cation) in different proportions, with the intention to obtain a performance enhancement in the DSSCs.

2 Experimental

2.1 Materials

Polyacrylonitrile (PAN), CsI, LiI, iodine (I_2), ethylene carbonate (EC), and propylene carbonate (PC) all with purity greater than 98 %, purchased from Aldrich, were used as starting materials. Prior to use, CsI and LiI were vacuum dried for 4 h at 150 °C, and PAN was vacuum dried for 24 h at 50 °C. Conducting Fluorine doped tin oxide (FTO) glass with sheet resistance of 7 Ω cm^{-2} and sensitizing dye cis-diisothiocyanato-bis(2,2′-bipyridyl-4,4′-

Table 1 Mass fractions of LiI and CsI used to prepare the PAN-based polymer gel electrolytes, where the amount of PAN, EC, and PC were kept at 0.10, 0.40, and 0.40 g, respectively. Molar ratio of the salts and ionic strength of the electrolyte are also included

Electrolyte	*a*	*b*	*c*	*d*	*e*	*f*	*g*
CsI g	0.00	0.01	0.02	0.03	0.04	0.05	0.06
LiI g	0.06	0.05	0.04	0.03	0.02	0.01	0.00
I_2 g	0.0114	0.0105	0.0095	0.0086	0.0077	0.0068	0.0059
Mass ratio CsI:LiI	0:6	1:5	1:2	1:1	2:1	5:1	6:0
Molar ratio CsI:LiI	0.0:100	9.3:90.7	20.5:79.5	34.0:66.0	50.7:49.3	72.0:28.0	100:0.0
Ionic strength mol Kg^{-1}	0.46	0.42	0.39	0.35	0.31	0.28	0.24

dicarboxylato) ruthenium(II) bis(tetrabutylammonium) (N719) were purchased from Solaronix SA. TiO_2 P25 and P90 were from Degussa Germany.

2.2 Preparation of the gel electrolyte

A series of gel electrolytes were prepared by keeping the amount of PAN (0.10 g), EC (0.40 g), and PC (0.40 g) unchanged and varying the weight ratio of CsI and LiI according to the Table 1. The amount of iodine added was fixed at 0.1 times of the total moles of CsI + LiI.

All chemicals were mixed according to the detailed procedure described in [9]. This procedure yields a visually homogeneous and gel-type polymer electrolyte. The resulting gel was gently pressed between two cleaned glass plates to obtain a thin electrolyte membrane which was used for the fabrication of DSSCs.

2.3 Assembly of DSSCs

Two successive layers of TiO_2, each of about 5 μm thickness, were deposited on the conducting glass substrate in order to prepare the photo-anode. The first layer was prepared by grinding 0.5 g of P90 TiO_2 powder for ~30 min with ~2 ml of HNO_3 (pH 1) in a mortar. The resulting slurry was coated on the well-cleaned FTO glass substrate with a spin coater using a multi-speed program. The first stage was done at 1,000 rpm for 2 s and the second stage at 2,300 rpm for 60 s. During the spin-coating, a part of the glass plate was covered with an adhesive tape to prevent coating on the part needed for electrical contacts. After drying in air for ~30 min, the coated TiO_2 electrode was sintered at 450 °C for ~30 min in air. Subsequently, the second layer of TiO_2 was coated on the first layer by using Degussa P25, TiO_2 powder. For the preparation of this layer, 0.5 g of TiO_2 powder was ground well for ~30 min with ~2 ml of HNO_3 (pH 1) in an mortar. The resulting colloidal suspension was diluted to get a 5 % (*w/w*) solution, and subsequently, it was stirred overnight at 60 °C and 25 % (*w/w*) solution was obtained. Subsequently, ~0.1 g of Carbowax and few drops of Triton X 100 (surfactant) were added and mixed well. This colloidal suspension was casted using the doctor blade method followed by sintering in air at 450 °C for 30 min to obtain a porous TiO_2 layer. The final film thickness was ~10 μm. The adsorption of sensitizing dye was carried out by soaking the TiO_2-coated glass plates in an ethanolic solution of the dye while both were hot (~60 °C) and kept for 24 h followed by rinsing with acetone.

The DSSCs were assembled by sandwiching the gel electrolyte film between the sensitized-TiO_2 electrode and the counter electrode which is a glass plate coated with platinum (Pt).

2.4 Characterization

Complex impedance measurements were made on gel electrolyte samples with a thickness of ~0.5 mm sandwiched between two stainless (SS) steel electrodes of 10.5-mm diameter, using a computer-controlled HP 4192 impedance analyzer in the frequency range of 10 Hz–10 MHz. Prior to measurements, the samples were heated to 60 °C and thereafter the temperature of the sample was varied from 60 to 0 °C, and the measurements were taken at 5 °C intervals. During impedance measurements, SS/electrolyte/SS cells were kept inside a Faraday cage (hollow metal cylinder), and the temperature was controlled by using a water bath connected to a GRANT heating system (type KD, England) and a cooling system (HETOIFRIGE, Denmark). A thermocouple connected to a HEWLETT PACKARD 344401A multimeter was used to measure the sample temperature.

DSC thermograms of the electrolyte samples were obtained by using a Mettler Toledo DSC 30 differential scanning calorimeter. Each sample was scanned at a rate of 10 °C min^{-1} from −140 to 100 °C. The measurements were carried out by performing several consequent heating and cooling cycles with the same sample. A flow of nitrogen gas was continuously purged to the sample in order to avoid contact with atmospheric moisture.

For the solar cells characterization, fabricated DSSCs were irradiated by a LOT-Oriel GmbH solar simulator 1.5 AM, 1,000 Wm^{-2}. *I–V* characteristics of the cells were

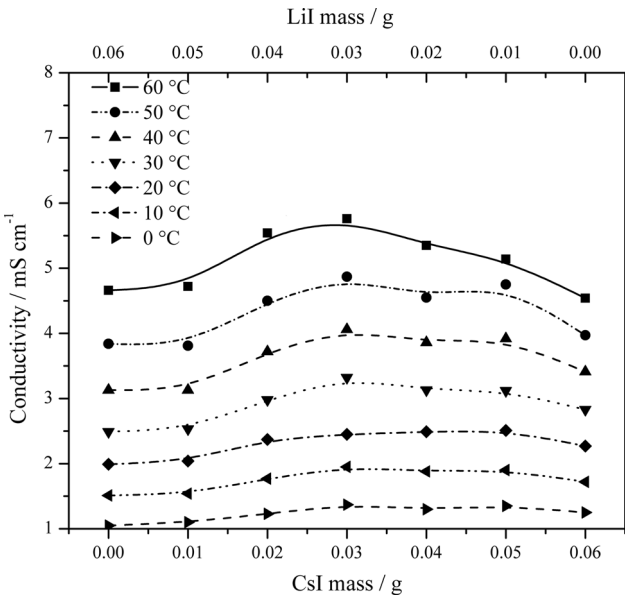

Fig. 1 Variation of conductivity against salt composition in the system PAN:EC:PC: CsI/LiI. Sample labeling is given in Table 1, and details about conductivity measurements and calculations are given in Sect. 2.4

obtained using a computer-controlled eDAQ Potentiostat and e-coder. Effective area of the cell was 11 mm^2.

3 Results and discussion

3.1 Conductivity of the gel polymer electrolyte

The variation of conductivity versus salt composition of the electrolytes at different temperatures is shown in Fig. 1. All the gel polymer electrolyte samples fabricated in this work showed conductivities of the order of milli Siemens per cm (S cm^{-1}) in the temperature range 0–60 °C. The electrolyte containing the mass ratio, CsI:LiI = 1:1, showed the highest conductivity out of all the samples studied in the entire temperature range measured. This sample (*d*) exhibited conductivity values of 1.37×10^{-3}, 2.94×10^{-3}, and 4.87×10^{-3} S cm^{-1} at 0, 25, and 50 °C, respectively. It should be noted, however, that the effect on the conductivity with the varying salt mass ratio is small. However, the electrolyte sample having only LiI (sample *a*) exhibited the lowest conductivity values of 1.05×10^{-3}, 2.24×10^{-3}, and 3.84×10^{-3} S cm^{-1} at 0, 25, and 50 °C, respectively. The electrolyte sample (*g*), a sample with CsI alone and without LiI, exhibited better conductivities than that of the electrolyte containing LiI only (sample *a*) as the salt. The electrolyte sample (*g*) exhibited conductivity values of 1.25×10^{-3}, 2.55×10^{-3}, and 3.97×10^{-3} S cm^{-1} at 0, 25, and 50 °C, respectively.

In the literature, conductivity values comparable to those of the present system have been reported for PAN-/EC-/PC-based gel polymer electrolytes systems containing different iodide salts [9, 19]. For example, it was reported that the conductivity of Hex_4NI containing PAN-based electrolytes is higher than that containing MgI [9], and subsequently, the conductivity of systems containing LiI is higher than that of Hex_4NI-based systems [19]. Hence, according to literature, highest conductivity for PAN-/EC-/PC-based single-salts gel is shown with LiI. However, in the present work, the system with CsI as the only ionic salt has shown higher conductivity that that of LiI-containing sample. Thus, CsI can incur higher conductivity for single-salt systems compared to other studied salts. The comparison of these conductivities is done for temperatures below 50 °C.

In the present electrolyte system, there are three types of mobile ions namely I^-, Cs^+, and Li^+. The ionic radii of these ions are about 2.2, 1.67, and 0.59 Å, respectively [20]. The lower conductivity shown by sample (*a*) with LiI only as the salt can be due to the limiting of ionic mobility by the stronger interactions among ionic species from the cation and the functional groups in the polymer and in the plasticisers EC and PC in addition to formation of triple ions [21, 22]. In sample *a*, there are no Cs^+ ions; thus, the available ionic species are Li^+ and I^- ions. Since the Li^+ ion has high charge density, it can be strongly coordinated with the electronegative sites in the electrolyte. Further, Li^+ ions can cross-link long polymer chains reducing the flexibility of the electrolyte which can hinder the ionic mobility. This may be the reason for obtaining the lowest conductivity for sample *a*. With added amounts of CsI, the conductivity starts to increase gradually up to a maximum at salt composition CsI:LiI wt. ratio 1:1. This can be due to contributions from several competing factors such as the higher salt dissociation owing to the larger size of the Cs^+, the flexibility incurred by the polymer matrix due to a reduced number of strong cross linking centers with decreasing amount of Li^+ ions and disorder imposed by the presence of ionic species of different sizes. After reaching the maximum at CsI:LiI = 1:1, conductivity gradually drops with further addition of CsI. This is very likely due the formation of higher ionic aggregates. In general, the conductivity enhancement obtained for mixed salt systems up to an optimum concentration can also be attributed to the disorder imposed to the polymer matrix by the presence of large and small cations in the system.

The conductivity appears to follow the Vogel-Tammann-Fulcher (VTF) or super-Arrhenius [19, 23] type behavior with increasing temperature. Hence, the data were fitted to the VTF equation:

$$\sigma(T) = AT^{-1/2} \exp\left[-E_a/k_B(T - T_0)\right], \quad (1)$$

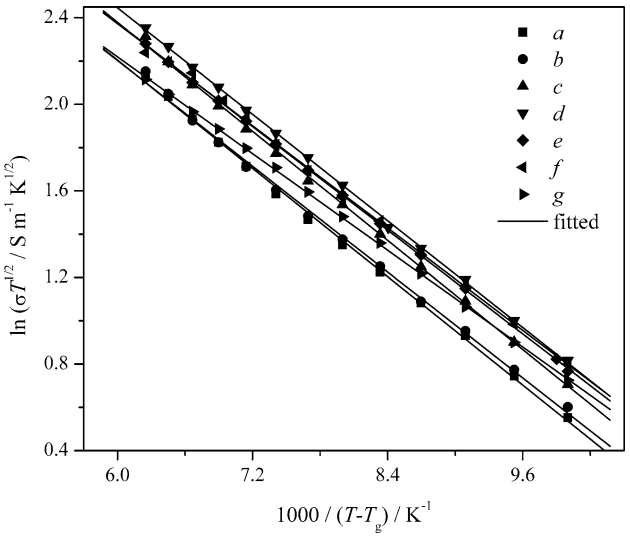

Fig. 2 Variation of $\sigma T^{1/2}$ plotted against 1,000/(T–T_g) for different salt composition ratios CsI/LiI in the system PAN:EC:PC:CsI/LiI. The symbols are experimental data, and each *solid line* is fitted curve to VTF equation

where E_a is the Pseudo-activation energy, A is the pre-exponential factor, and k is Boltzmann constant. The pseudo-activation energy E_a can be related to polymer segmental motion, which is associated with the mobility of charge carriers. T_0 is a reference temperature, called the ideal glass transition temperature, usually associated with the temperature at which the free volume disappears. In this study, the measured glass transition temperature (T_g) was taken as T_0 as the ideal glass transition temperature, and the appropriateness of this selection is manifested by the better fitting as shown in Fig. 2. The calculated E_a and pre-exponential factors are given Table 2. An activation energy value close to 35 meV is exhibited by all the samples, although a trend of activation energy decrease is shown for increasing amounts of CsI. Because of the small variations exhibited, it is difficult to interpret the behavior of E_a values for mixed systems very clearly. However, the difference in E_a values of the end samples is quite clear. The conductivity enhancement shown by sample *g* compared to sample *a,* is reflected by a drop of E_a (sample *a*) from 36 to 32 meV when LiI is replaced by CsI. Since the pre-exponential factor, A, is related to the charge carrier density, the drop shown for the factor A from 110.6 to 85.8 S m^{-1} K$^{1/2}$ when LiI is replaced by CsI can be attributed to a decrease of charge carrier density. Note also that the molar concentration of CsI is less than that of LiI since the molar weight of LiI is smaller than that of CsI. As a consequence, the trend of A follows the trend of the conductivity.

Table 2 Glass transition temperature, T_g, pre-exponential factor, A, and the activation energy, E_a, for electrolytes containing different mass fractions of CsI and LiI. A and E_a values were extracted from the linear fitting using $\sigma T^{1/2}$ vs 1,000/(T–T_g) plot

Sample	CsI:LiI (wt. ratio)	T_g/ °C	A/S (m^{-1} K$^{1/2}$)	E_a (meV)
a	0:6	−100.25	110.6	36
b	1:5	−100.87	104.2	35
c	1:2	−100.91	134.1	36
d	1:1	−102.95	135.1	35
e	2:1	−100.50	118.0	34
f	5:1	−100.49	113.7	34
g	6:0	−100.17	85.8	32

3.2 Density and mobility of charge carriers

In order to understand the conductivity in electrolyte samples, the charge carrier density and mobility were calculated using a newly developed method by means of complex impedance data [24]. The frequency dependence of the real and imaginary parts of the complex dielectric functions was calculated using the following equations:

$$\varepsilon'_r = \frac{-Z''}{\omega C_o (Z'^2 + Z''^2)}, \tag{2}$$

$$\varepsilon''_r = \frac{Z'}{\omega C_o (Z'^2 + Z''^2)}, \tag{3}$$

where Z', Z'', ω, and C_o are real and imaginary parts of the impedance, angular frequency, and geometric capacitance of the cell. Then the dielectric loss tangent was calculated by

$$\tan\phi = \frac{\varepsilon''}{\varepsilon'} = -\frac{Z'}{Z''}. \tag{4}$$

According to the method described in [24, 25], the effective dielectric constant of the electrolyte sandwiched between two blocking electrodes is given by

$$\tilde{\varepsilon}* = \varepsilon'_\infty \left\{ \left(1 + \frac{\delta}{1 + (\omega\tau_m)^2 \delta} \right) - i \left(\frac{\omega\tau_m \delta^{3/2}}{1 + (\omega\tau_m)^2 \delta} \right) \right\}, \tag{5}$$

where ε'_∞ is the high frequency permittivity, $\tilde{\varepsilon}*$ the effective complex dielectric constant, ω, the angular frequency of the signal, δ a constant and τ_m is the relaxation time corresponding to the maximum dielectric loss tangent. The constant δ in Eq. (5) is given by

$$\delta = \frac{d}{(D\tau_m)^{1/2}} = \frac{d}{\lambda}, \tag{6}$$

where D is the diffusion coefficient, d *is* half the sample thickness, and λ is the Debye length. Therefore, the dielectric loss tangent, tan ϕ, can be obtained from

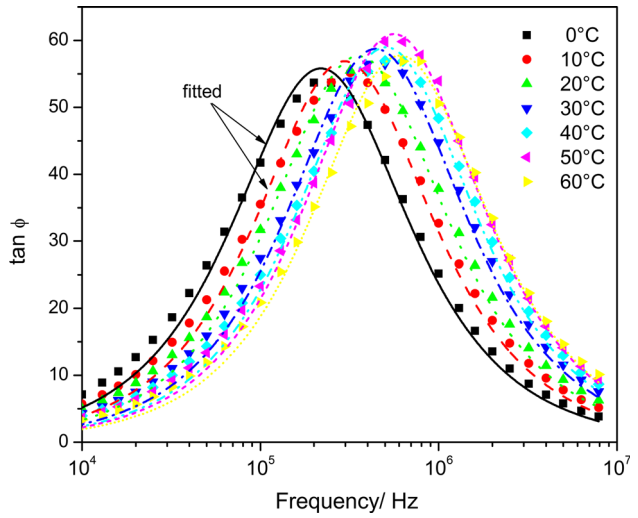

Fig. 3 Variation of Dielectric loss tangent against frequency for salt composition ratio CsI:LiI = 1:1 in the PAN:EC:PC:CsI/LiI electrolyte at different temperatures. *Point symbols* represent measured data whereas *line symbols* represent *fitted curves*. Even though measurements were taken at 5 °C in the frequency range 10 Hz–10 MHz, the figure shows data only for 10 °C intervals in a limited frequency range close to the maximum for better clarity

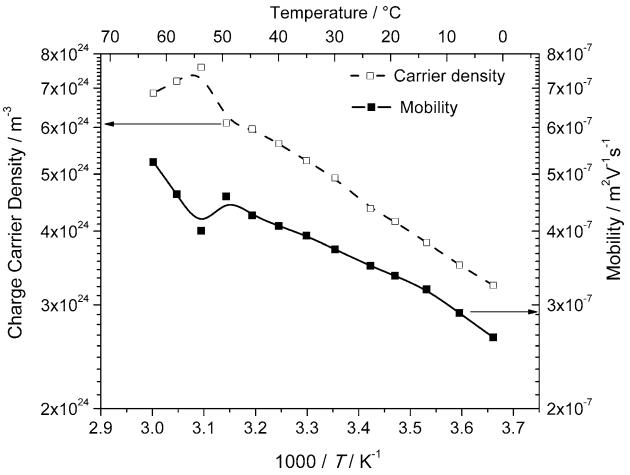

Fig. 4 Variation of charge carrier density and mean mobility of charge carriers against reciprocal temperature for the salt composition CsI:LiI = 1:1 in the PAN:EC:PC:CsI/LiI electrolyte

$$\tan(\phi) = \frac{\omega\tau_m\sqrt{\delta}}{1+\omega^2\tau_m^2} \tag{7}$$

using that δ is very much greater than one ($d \gg \lambda$) since λ is about few nanometers, and the sample thickness in this study is about 1 mm [26]. The Nernst–Einstein relation gives the relationship between the mobility and the diffusion coefficient, D,

$$\mu = \frac{eD}{k_B T} \tag{8}$$

and μ can be determined using Eqs. (6) and (8) giving

$$\mu = \frac{ed^2}{k_B T \tau_m \delta^2} \tag{9}$$

Thus, n can be determined using $\sigma = ne\mu$.

$$n = \frac{\sigma k_B T \tau_m \delta^2}{e^2 d^2} \tag{10}$$

The measured dielectric loss tangent against frequency for salt composition CsI:LiI = 1:1 in the PAN:EC:PC:CsI/LiI electrolyte is shown in Fig. 3. In order to calculate the mobility and the charge carrier density, parameters δ and τ_m were determined by fitting the measured dielectric loss tangent to the model Eq. (7). The lines in Fig. 3 show fit to the frequency dependence of dielectric loss tangent. Very good fits to the equation were obtained in this work justifying the appropriateness of the equation. For better clarity in Fig. 2, only the data for 10 °C intervals and a limited frequency range close to the maximum are shown, even though the measurements and fittings were done at 5 °C intervals for a frequency range 10 Hz–10 MHz.

The calculated mobility and charge carrier density for the highest conductivity electrolyte sample (sample *d*) are shown in Fig. 4. Both the mobility and carrier density increase with increasing temperature. The results clearly indicate that the conductivity increases with increasing temperature in this amorphous electrolyte evidently due to an increase in both density and mobility of charge carriers. The slight decrease of carrier density shown for temperatures higher than 55 °C can be attributed to the loss of I_2 from the electrolyte by evaporation at high temperatures. On the other hand, the results of rheological measurements done for comparable PAN-EC-PC gels suggest a structural change of the type "strong-to-weak" at about 60 °C [27]. Thus, such a structural change can influence the mobility and carrier density anomaly shown around 50–60 °C. The variation of number density and mobility of charge carriers as a function of 1,000/T for sample *a*, and *g* (single-salt systems) are shown in Fig. 5. Sample *a* (sample with LiI only) has shown lower mobility values than that of the sample *g* (sample with CsI only). Conversely, Sample *a* (sample with LiI only) has shown higher carrier density values than that of the sample *g* (sample with CsI only) and compensated possible effect to the ionic conductivity. Since sample *a* has the highest ionic strength as shown in the Table 1, higher carrier density shown by sample *a* can be understand. An abrupt mobility increase and carrier density decrease are shown for sample *a* at 35 °C. Similar behavior is exhibited by sample *g* around 15 °C. This can possibly be due ionic interactions, but in this work, we did not intend to do a detailed understanding of this behavior

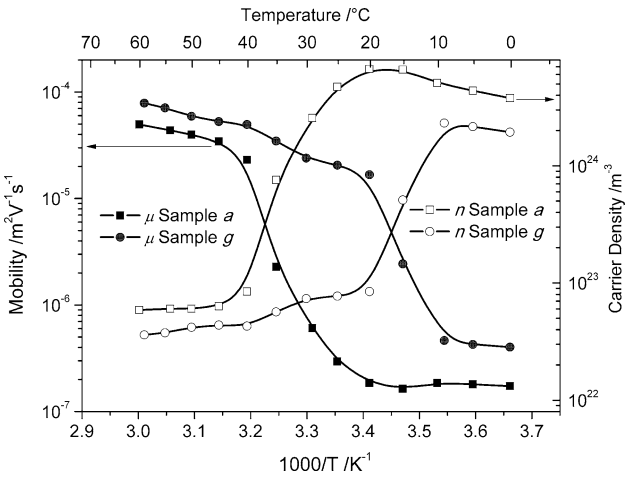

Fig. 5 The variation of density and mean mobility of charge carriers against 1,000/T for sample *a* and sample *g*

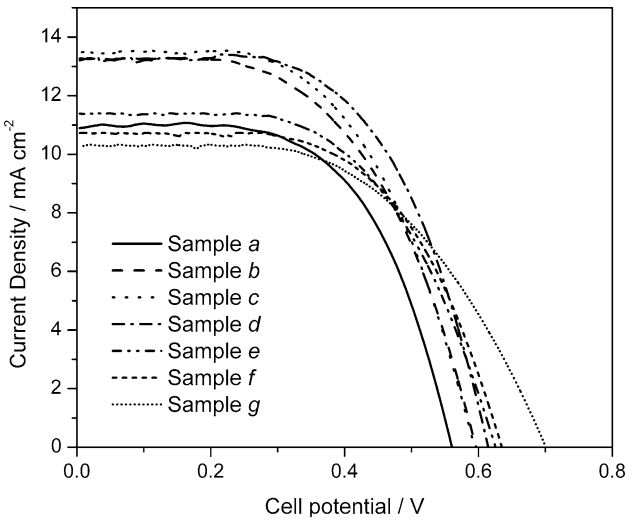

Fig. 6 Photocurrent density vs. voltage (*J-V*) characteristics of seven quasi-solid state dye-sensitized solar cells fabricated with different LiI:CsI salt mass ratios in the electrolyte

since our major focus is efficiency enhancement in solar cells. However, in order to better understand the mobility and carrier density variation, the work is in progress by using electrochemical methods and rheological measurements.

3.3 Characterization of dye-sensitized solar cells

The photocurrent density versus photovoltage (*J-V*) characteristics of seven solar cells of configuration Glass/FTO/TiO_2/Dye/electrolyte/Pt/FTO/glass were measured using gel polymer electrolyte samples with seven different LiI/CsI salt mass fractions (samples *a* to *g*). The (*J-V*) characteristics curves for all the seven sells are shown in Fig. 6.

Table 3 Parameters of solar cells with PAN/EC/PC gel electrolytes of different LiI:CsI mass fractions

Electrolyte	CsI:LiI (wt. ratio)	V_{oc} (mV)	J_{sc} (mA cm^{-2})	*FF* (%)	η (%)
a	0:6	560	10.9	59.8	3.6
b	1:5	596	13.3	54.3	4.3
c	1:2	594	13.5	55.9	4.5
d	1:1	614	13.2	58.9	4.8
e	2:1	626	11.4	56.9	4.1
f	5:1	636	10.7	58.7	4.0
g	6:0	700	10.3	54.4	3.9

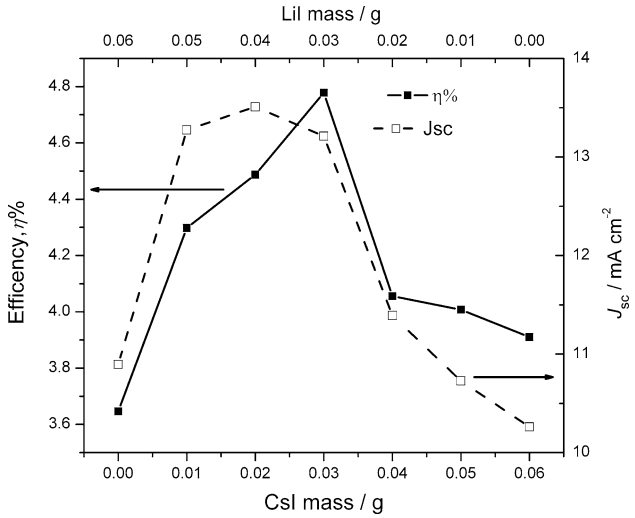

Fig. 7 Variation of efficiency (η) and short-circuit current density (J_{sc}) of all seven solar cells as a function of the weight of LiI (*bottom x* axis) and weight of CsI (*top x* axis)

Solar cell parameters such as the open circuit voltage (V_{oc}) and the short-circuit current density (J_{sc}) were noted, and the fill factor (*FF* %) and efficiency (η %) were calculated for all the cells studied, and the results are tabulated in Table 3. The equations for calculating *FF* % and η % can be found from the literature [9, 19].

The efficiency, η, and the short-circuit current density, J_{sc}, as a function of the weight of LiI (bottom *x* axis) and weight of CsI (top *x* axis) are shown in Fig. 7 for all the seven solar cells. The efficiency variation generally follows the variation of J_{sc} for all except for sample *c*. The most important observation made in this study is that all cells with binary iodides have shown a performance enhancement compared to that of the single-salt systems except for the slightly lower J_{sc} value shown for sample *f* compared to sample *a*. This clearly highlights the advantage of incorporating binary iodides for the electrolytes intended for DSSCs.

Short-term stability of the cell was measured for 3 days, and no significant efficiency drop is observed. A small drop of J_{sc} is observed with aging but it is compensated by the increase of V_{oc} resulting in unchanged efficiency. In addition, further work is continuing in order to investigate the long term stability of the cells under real outdoor conditions.

The highest energy conversion efficiency of 4.8 % is shown by the electrolyte with LiI :CsI weight ratio 1:1 (sample *d*). The cells with electrolyte containing LiI alone (sample *a*) and CsI alone (sample *g*) as the salt have efficiencies of 3.6 and 3.9 %, respectively. Thus, the use of the binary iodide mixture has clearly enhanced the solar cell efficiency by about 23 %. It is interesting to note that the highest solar cell efficiency corresponds to the maximum conductivity salt composition (Fig. 1) and that the efficiency variation with salt composition more or less follows the variation of short-circuit photocurrent density (J_{sc}) as shown in Fig. 7. However, the maximum J_{sc} of 13.5 mA cm^{-2} is achieved by the solar cell with electrolyte having CsI:LiI weight ratio of 1:2 (sample *c*), whereas the most efficient cell which contains electrolyte sample *d* (CsI:LiI = 1:1) records very close value (13.2 mA cm^{-2}). Solar cells with single-salt electrolytes (sample *a* and sample *g*) have shown J_{sc} of about 10.9 and 10.3 mA cm^{-2}. Thus, the use of the binary iodide mixture has clearly enhanced the J_{sc} of solar cells with the maximum enhancement of about 24 %.

The correlation between the solar cell efficiency and the ionic conductivity as evidenced by Figs. 1 and 7 suggests that the dominant contribution to the solar cell efficiency has come from the J_{sc} and is determined essentially by the relative amount of iodide ion conductivity in the gel electrolyte. However, as illustrated in Fig. 7 the highest J_{sc} values are shown by sample *c* (and not *d*) which contains more LiI by weight than CsI. Besides when J_{sc} curves (Fig. 7) are scrutinized and compared with conductivity curves in Fig. 1, it is clearly understood that comparatively higher J_{sc} values are shown by cells containing more LiI than CsI. For instance, DSSCs with sample *a* and *b* have higher J_{sc} than expected from the conductivity data highlighting the advantage of incorporation Li^+ into the electrolyte system. This effect (higher J_{sc}, for more LiI-containing sample) can be attributed to the other effects, such as increase of electron injection rates, reduction of back electron transfer (apart from conductivity of redox mediator) imposed by the smaller Li^+ cation in the electrolyte.

The Influence of Li^+ ions to enhance J_{sc} of DSSCs has been observed by many investigators. Shi et al. [28] found that the short-circuit photocurrents of DSSCs gradually increase with decreasing cation size resulting in the highest J_{sc} for LiI-containing electrolytes, and the behavior was attributed to an increase of the electron injection rates. Li et al. [29] also observed a J_{sc}, increase with increasing amounts of Li^+ compared to the dimethylimidazolium cation (DMI^+). The same authors correlated this phenomenon to a strong retardation of the interfacial charge recombination ability of adsorbed lithium cations to TiO_2 compared to that of adsorbed dimethylimidazolium cations, contributing to an over one order of magnitude enhancement of the electron diffusion length. Pelet et al. [30] have shown that faster dye regeneration kinetics can be observed when smaller cations such as Li^+ or Mg^{2+} are present in the electrolytes and contribute to the J_{sc} enhancement. Thus, the J_{sc} enhancement with increasing amount of LiI can be the result of faster electron injection rates and dye regeneration rates.

The J_{sc} and V_{oc} variation on the type and the nature of the cation are due to interfacial kinetics of the dyed TiO_2 film, and a study of shift of flat-band potentials due to small and large cation was reported [6]. When a DSSC irradiated with sun light, the injected electrons from the excited dye molecules are accumulated at the conduction band of TiO_2, and consequently the cations in the electrolyte are adsorbed into the TiO_2 film. The V_{oc} is governed by the relative positions of the flat-band potential, and the redox potential of the electrolyte for instance adsorbed cations can move flat-band potential of TiO_2 positively resulting in a drop in photovoltage of the cell [6]. Thus, adsorbed small cations onto the porous TiO_2 can decline the V_{oc} of the cell. Therefore, the decrease in V_{oc} caused by adsorption of cations is pronounced for the DSSC with LiI only (V_{oc} = 560 mV for sample *a*) compared to that for the DSSC with CsI alone (V_{oc} = 700 mV for sample *g*). Conversely, the positive shift of the TiO_2 flat-band potential inspires the charge injection from the excited dye molecules to TiO_2 causing a lower photovoltage and higher photocurrent.

Conversely to the effect of smaller cations, larger cations in the electrolytes can contribute to a V_{oc} enhancement. For an example, an open circuit voltage increase with the increasing radius of the alkali metal cation series Li^+, Na^+, K^+, Rb^+, and Cs^+ has been observed for dye-sensitized solar cells containing PEO-based gel electrolytes [17]. These results were attributed to a shift of the electron Fermi level. This effect is valid also for liquid type electrolytes, and a very clear increase of V_{oc} and fill factor have been observed for dye-sensitized solar cells in the order of $Li^+ < Na^+ < K^+ < DMI^+$ [28]. Using impedance data analysis, the increase of the cell photovoltage is mainly correlated to an upward shift of the conduction band edge induced by the adsorption of low-charge-density cations on the surface of TiO_2 nanocrystals. Thus, that the increasing trend of V_{oc} with the size of the cation in the electrolyte is due to a reduction of the charge recombination is already established. The results observed for the photocurrents and photovoltages in this study for end members, *i.e.*, cells with sample *a* and *g*, agree with the results and mechanisms discussed above for related systems. The combined effect of two competing trends for small and large cations (small cations contribute to enhance J_{sc} and large cations contribute to

enhance V_{oc}) has thus contributed to the efficiency enhancement obtained for these mixed salt systems.

4 Conclusions

This paper reports for the first time, the mixed cation effect of using a binary alkaline iodide system consisting of a small alkali cation (Li^+) and a large cation (Cs^+) in a PAN-based quasi-solid state electrolyte on the DSSC performance. The analysis of complex impedance measurements shows that the conductivity of the electrolyte can be enhanced by using the binary mixtures of two iodide salts. The electrolyte with the binary mixture of CsI:LiI = 1:1 mass ratio shows the highest conductivity of 2.94×10^{-3} S cm^{-1} at 25 °C. The disorder produced by the variation of the cross-linked transient bonds may also facilitate the ion transport. Both the density and the mobility of the charge carriers have contributed to the temperature dependence of the conductivity of the electrolytes.

Even though J_{sc} in general is determined by the I^- ion conductivity, the incorporation of a small alkaline cation in the system has another effect, facilitating the injection of electrons into TiO_2 and the dye regeneration. This is shown by the shift of the maximum of J_{sc} toward higher Li content samples. As reported by other groups, a noticeable trend of J_{sc} enhancement is observed with increasing charge density (i.e., small cations), and V_{oc} is improved by decreasing charge density (i.e., large cations).

The electrolyte containing LiI:CsI with mass ratio 1:1 showed the best solar cell performance highlighting the influence of the mixed cation system in the electrolyte on the performance of the cell with an enhanced energy conversion efficiency of $\sim$4.8 % under the irradiation of one sun. This enhancement comes from two competing effects by two dissimilar cations (Li^+ and Cs^+) influencing the electron injection rates and dye regeneration and contributions to transport of the redox mediator. The use of binary mixtures of alkyl iodides has given a 23 % efficiency enhancement and a 24 % short-circuit-current density enhancement. This work reveals the usefulness of employing a binary alkyl iodide mixture (instead of a single cation iodide) to achieve a significant efficiency enhancement in different types of dye-sensitized solar cells systems.

Acknowledgments Authors wish to thank the National Research Council (NRC) of Sri Lanka (Grant 11-196), and the Swedish Research Council (SRC) for research support.

References

1. Bella F, Bongiovanni R (2013) Photoinduced polymerization: an innovative, powerful and environmentally friendly technique for the preparation of polymer electrolytes for dye-sensitized solar cells. J Photochem Photobio C 16:1–21
2. Chatzivasiloglou E, Stergiopoulos T, Kontos AG, Alexis N, Prodromidis M, Falaras P (2007) The influence of the metal cation and the filler on the performance of dye-sensitized solar cells using polymer-gel redox electrolytes. J Photochem Photobio A 192:49–55
3. Huo Z, Dai S, Wang K, Kong F, Zhang C, Pan X, Fang X (2007) Nanocomposite gel electrolyte with large enhanced charge transport properties of an I_3/I redox couple for quasi-solid-state dye-sensitized solar cells. Sol Energy Mater Sol Cell 91:1959–1965
4. Lee K-M, Suryanarayanan V, Ho K-C (2009) Influences of different TiO_2 morphologies and solvents on the photovoltaic performance of dye-sensitized solar cells. J Power Sources 188: 635–641
5. Yella A, Lee HW, Tsao HN, Yi C, Chandiran AK, Nazeeruddin MK, Diau EW-G, Yeh C-Y, Zakeeruddin SM, Grätzel M (2011) Porphyrin-sensitized solar cells with cobalt (II/III)-based redox electrolyte exceed 12 percent efficiency. Science 334:629–634
6. Dissanayake MAKL, Thotawatthage CA, Senadeera GKR, Bandara TMWJ, Jayasundara WJMJSR, Mellander B-E (2013) Efficiency enhancement in dye sensitized solar cells based on PANgel electrolyte with $Pr_4NI + MgI_2$ binary iodide salt mixture. J Appl Electrochem 43:891–901
7. Kelly CA, Farzad F, Thompson DW, Stipkala JM, Meyer GJ (1999) Cation-controlled interfacial charge injection in sensitized nanocrystalline TiO_2. Langmuir 15:7047–7054
8. Bandara TMWJ, Jayasundara WJMJSR, Dissanayake MAKL, Furlani M, Albinsson I, Mellander B-E (2013) Effect of cation size on the performance of dye sensitized nanocrystalline TiO_2 solar cells based on quasi-solid state PAN electrolytes containing quaternary ammonium iodides. Electrochim Acta 109:609–616
9. Bandara TMWJ, Dissanayake MAKL, Jayasundara WJMJSR, Albinsson I, Mellander B-E (2012) Efficiency enhancement in dye sensitized solar cells using gel polymer electrolytes based on a tetrahexylammonium iodide and MgI_2 binary iodide system. Phys Chem Chem Phys 14:8620–8627
10. Kambe S, Nakade S, Kitamura T, Wada K, Yanagida S (2002) Influence of the electrolytes on electron transport in mesoporous TiO_2-electrolyte systems. J Phys Chem B 106:2967–2972
11. Kopidakis N, Schiff EA, Park N-G, van de Lagemaat J, Frank AJ (2000) Ambipolar diffusion of photocarriers in electrolyte-filled, nanoporous TiO_2. J Phys Chem B 104:3930–3936
12. K. Kalyanasundaram (2010) EPFL Press, pp. 121–123
13. Grätzel M (2001) Photoelectrochemical cells. Nature 414:338–344
14. Kang J, Li W, Wang X, Lin Y, Li X, Xiao X, Fang S (2004) Gel polymer electrolytes based on a novel quaternary ammonium salt for dye-sensitized solar cells. J Appli Electrochem 34(3):301–304
15. Dissanayake MAKL, Thotawatthage CA, Senadeera GKR, Bandara TMWJ, Jayasundara WJMJSR, Mellander B-E (2012) Efficiency enhancement in dye sensitized solar cells based on PAN gel electrolyte with $Pr_4NI + MgI_2$ binary iodide salt mixture. J Photochem Photobio A 246:29–35
16. Tennakone K, Senadeera GKR, Perera VPS, Kottegoda IRM, Silva LAAD (1999) Dye-sensitized photoelectrochemical cells based on porous SnO_2/ZnO composite and TiO_2 films with a polymer electrolyte. J Chem Mater 11:2474–2477
17. Shen X, Xu W, Xu J, Liang G, Yang H, Yao M (2008) Quasi-solid-state dye-sensitized solar cells based on gel electrolytes containing different alkali metal iodide salts. Solid State Ion 179:2027–2030
18. Hoshikawa T, Ikebe T, Kikuchi R, Eguchi K (2006) Effects of electrolyte in dye-sensitized solar cells and evaluation by impedance spectroscopy. Electrochim Acta 51:5286–5294
19. Bandara TMWJ, Jayasundara WJMJSR, Dissanayake MAKL, Fernando HDNS, Furlani M, Albinsson I, Mellander B-E (2014)

Quasi solid state polymer electrolyte with binary iodide salts for photo-electrochemical solar cells. J Hydrogen Energy 39: 2997–3004
20. Atkins PW (1994) Physical chemistry, 5th edn. Oxford University Press, Oxford, p C24
21. Ugur MH, Toker RD, Kayaman-Apohan N, Güngör A (2014) Preparation and characterization of novel thermoset polyimide and polyimide-peo doped with LiCF3SO3. Express Polymer Lett 8:123–132
22. Dias FB, Plomp L, Veldhuis JBJ (2000) Trends in polymer electrolytes for secondary lithium batteries. J Power Sources 88:169–191
23. Vogel H (1921) The law of the relation between the viscosity of liquids and the temperature. Phys Z 22:645
24. Bandara TMWJ, Dissanayake MAKL, Albinsson I, Mellander B-E (2011) Mobile charge carrier concentration and mobility of a polymer electrolyte containing PEO and $Pr_4N^+I^-$ using electrical and dielectric measurements. Solid State Ion 189:63–68
25. Bandara TMWJ, Mellander B-E (2011) Evaluation of mobility, diffusion coefficient and density of charge carriers in ionic liquids and novel electrolytes. In: Kokorin Alexander (ed) Ionic liquids theory properties new approaches. InTech, Rijeka, pp 383–406
26. Bohinc K, Kralj-Iglic V, Iglic A (2001) Thickness of electrical double layer. Effect of ion size. Electrochim Acta 46:3033–3040
27. Dintcheva NTz, Furlani M, Jayasundara WJMJSR, Bandara TMWJ, Mellander B-E, La Mantia FP (2013) Rheological behavior of PAN-based electrolytic gel containing tetrahexylammonium and magnesium iodide for photoelectrochemical applications. Rheol Acta 52(10–12):881–889. doi:10.1007/s00397-013-0727-1
28. Shi Y, Wang Y, Zhang M, Dong X (2011) Influences of cation charge density on the photovoltaic performance of dye-sensitized solar cells: lithium, sodium, potassium, and dimethylimidazolium. Phys Chem Chem Phys 13:14590–14597
29. Li R, Liu D, Zhou D, Shi Y, Wang Y, Wang P (2010) Influence of the electrolyte cation in organic dye-sensitized solar cells: lithium versus dimethylimidazolium. Energy Environ Sci 3(11):1765–1772
30. Pelet S, Moser JE, Gratzel M (2000) Cooperative effect of adsorbed cations and iodide on the interception of back electron transfer in the dye sensitization of nanocrystalline TiO_2. J Phys Chem B 104:1791